

Low-energy electron diffraction analysis of the structure of a Cs-O/Ru(0001) coadsorbate phase

H. Over, H. Bludau, M. Skottke-Klein,* W. Moritz,[†] and G. Ertl

Fritz-Haber-Institut der Max-Planck-Gesellschaft, Faradayweg 4-6, D-1000 Berlin 33, Federal Republic of Germany

(Received 2 March 1992; revised manuscript received 22 June 1992)

The structure of the $(\sqrt{3}\times\sqrt{3})R30^\circ$ overlayer formed by coadsorption of Cs and O atoms ($\theta_{\text{Cs}}=\theta_{\text{O}}=0.33$) on a Ru(0001) surface was determined by low-energy electron diffraction. Both adsorbates occupy hcp-type hollow sites. If compared with the structures of the respective pure adsorbate phases, the bond lengths are modified in a way consistent with an effective transfer of electronic charge from Cs to O.

The properties of alkali metal and oxygen overlayers coadsorbed on transition metal surfaces have already been the subject of numerous investigations,¹ not only because of fundamental interest but also for the role played by these systems as actual promoters in catalytic reactions such as, e.g., ammonia synthesis.² Apart from the formation of a large variety of mixed phases with long-range order, the general tendency for thermal stabilization of the alkali-metal adlayer by the addition of oxygen is indicative of strong interactions between both adsorbates. So far, however, complete structural information has still been lacking, but will be reported here for a particular system, namely, the Cs-O-Ru(0001)- $(\sqrt{3}\times\sqrt{3})R30^\circ$ phase. The analysis was performed by low-energy electron diffraction (LEED), and represents one of a few successful determinations of the structural parameters of an atomic coadsorbate system using this technique. The first LEED-structural analysis of coadsorbed atoms was performed for Na and S on Ni(100) by Andersson and Pendry.³

The experiments were performed with a UHV system which was equipped with a display type four grids LEED optics and with standard facilities for surface cleaning and characterization, as described elsewhere in a report on the structural analysis of pure Cs/Ru(0001) overlayers.⁴

LEED intensity measurements were performed at normal incidence of the primary beam at a sample temperature of 100 K. A computer-controlled video camera was used to record integrated spot intensities of two integer and four fractional order beams (energy range 70–380 eV) from the fluorescence screen.⁵

Starting with an ordered Cs/Ru(0001)- $(\sqrt{3}\times\sqrt{3})R30^\circ$ structure with Cs coverage $\theta_{\text{Cs}}=0.33$, already addition of small doses of oxygen (0.05 L) led to the appearance of a new incommensurate superstructure and a successive disappearance of the $(\sqrt{3}\times\sqrt{3})R30^\circ$ pattern. This clearly indicates a strong interaction between oxygen and the Cs adsorbate layer. O₂ exposure between 0.3 and 0.9 L and subsequent annealing to a temperature of $T=310$ K, which is slightly above the onset of Cs desorption in the “clean” Cs/Ru(0001) phase, gives rise to the reappearance of a $(\sqrt{3}\times\sqrt{3})R30^\circ$ structure. During this annealing process no desorption of Cs atoms could be detected by means of Auger electron spectroscopy (AES) or thermal desorption spectroscopy. Therefore, the coexistence of patches of Cs- and Cs-O phases can be ruled

out. The oxygen coverage, which gives rise to a $(\sqrt{3}\times\sqrt{3})R30^\circ$ with highest intensity and lowest background was determined to be $\theta_{\text{O}}=0.35\pm 0.02$ (O₂ exposure: 0.7 L) by means of AES, measuring the peak-to-peak height of the signal of the O(*KLL*) Auger transition at 520 eV. The correlation between Auger signal and absolute O coverage was calibrated by combined AES and LEED measurements of the (2×2) and (2×1) phase of the system O/Ru(0001) with coverages $\theta_{\text{O}}=0.25$ and $\theta_{\text{O}}=0.50$, respectively. Hence, the unit cell of the $(\sqrt{3}\times\sqrt{3})R30^\circ$ -Cs/O phase contains one Cs and one O atom. The full width at half maximum sharpening of the fractional order beams in the Cs/O/Ru(0001) system as compared with the corresponding pure Cs/Ru(0001) system indicates an improved ordering in the coadsorbate system.

Theoretical *I/E* curves were calculated using the “layer doubling” method in combination with the “layer Korringa-Kohn-Rostocker” approach⁶ with extensive exploitation of symmetry relations both in real and reciprocal space.^{7,8} In the LEED program up to 9 spin-averaged phase shifts of Cs and Ru were used; alternatively 10 phase shifts of Cs were tested without exhibiting any noticeable effect on the *I/E* curves. Details about their computation can be found in Ref. 4. Oxygen phase shifts were taken from the literature⁹ which had been successfully applied in a previous LEED intensity calculation for Ni(110)-(2×1)O.¹⁰ All phase shifts were temperature corrected utilizing an effective Debye temperature of 420 K for bulk ruthenium layers, 80 K for the Cs [as adopted from our previous structural studies of the Cs/Ru(0001) system⁴] and 420 K for the oxygen surface layer; no attempt was made to optimize these parameters. The agreement between experimental and theoretical *I-E* data was quantified by the r_{DE} factor introduced by Kleinle *et al.*¹¹ and by Pendry's r_{P} factor.¹²

In this analysis the Cs-Ru, the O-Ru layer spacing, the first Ru-Ru layer spacing, a buckling in the second Ru layer, and the real part of the inner potential were simultaneously refined. For details concerning the procedure of the automatic structure refinement see Refs. 13 and 14. In addition, possible lateral relaxations within the topmost layer of the Ru substrate were included.

Starting point was the recently solved structure of the Cs/Ru(0001)- $(\sqrt{3}\times\sqrt{3})R30^\circ$ phase *without* coadsorbed O atoms.⁴ Here the Cs atoms occupy threefold coordinated hcp-type sites (i.e., with a Ru atom from the second

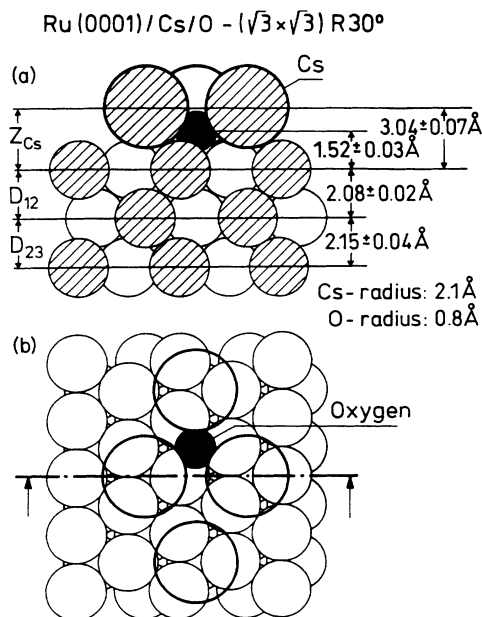


FIG. 1. Structure model for the Cs-O/Ru(0001)- $(\sqrt{3} \times \sqrt{3})R30^\circ$ coadsorbate phase. Large circles, Cs atoms; small solid circle, O atoms. (a) Side view [cut along the dash-dotted line of (b)]; (b) Top view. Structural parameters: $Z_{Cs} = 3.04 \pm 0.07$ Å; $Z_{Ox} = 1.52 \pm 0.03$ Å; $D_{12} = 2.08 \pm 0.02$ Å; $D_{23} = 2.15 \pm 0.04$ Å.

layer of the substrate just below the adsorbate) with the structural parameters $Z_{Cs} = 3.15 \pm 0.03$ Å, $D_{12} = 2.10 \pm 0.04$ Å, $D_{23} = 2.12 \pm 0.07$ Å (for nomenclature see Fig. 1). It had been found for this phase that I/E spectra calculated for any other type of adsorption site differ considerably from the experimental data. With the coadsorption system, on the other hand, the I/E curves recorded showed close similarities to those of the pure Cs($\sqrt{3} \times \sqrt{3})R30^\circ$ adlayer, obviously because the Cs atom is a much stronger scatterer than the O atom. It hence be-

TABLE I. r factors (r_{DE} and Pendry's r_P) for the best fit arrangement of the respective oxygen adsorption sites. Cs atoms occupy hcp sites.

r_{DE}	r_P	Adsorption site
0.33	0.31	hcp
0.43	0.47	bridge site
0.62	0.71	on top

same type of hcp sites. For the location of the O atom the following three high-symmetry positions may then be envisaged: (i) on top of a Cs atom, (ii) in a twofold symmetric bridge position across 2 Cs atoms, and (iii) in a threefold hollow site. With the former two configurations the positions of the oxygen nuclei would be above the plane formed by the Cs cores (for the reason of a very limited space for oxygen atoms) and as a consequence a substantial increase of the work function would be predicted. With the threefold hollow site, on the other hand, the O atom might be located even below the plane of Cs atoms (as actually is the case, as will be shown below), and hence the dipole moment and the work function change might exhibit the reverse sign, which would agree with the experimental findings.¹⁵

For the three Cs/O geometries sketched automatic structure refinements were performed, starting from different initial configurations in order to reach the corresponding local minimum in the hypersurface of the r_{DE} factor. These minima were typically reached after 6-7 iteration cycles, when the changes of the parameters attained values within the limits of 0.01 Å and 0.1 eV, respectively. The structural results of the fit procedure were confirmed by an r -factor analysis using Pendry's r factor r_P .¹² We found excellent agreement between r_{DE} and r_P as illustrated in Fig. 2. The optimum reliability factors r_P and r_{DE} are listed in Table I. The results strongly corroborate the above-made suggestion and clearly favor the hcp site as position for the O atom. The optimum r fac-

$(\sqrt{3} \times \sqrt{3})R30^\circ$ overlayer,⁴ which is attributed to the improved long-range order in the case of oxygen coadsorption. On top- and bridge-site occupancy of the O atoms can clearly be ruled out.

Somewhat to our surprise, the r factors turned out to be remarkably sensitive also to the vertical position of the O atom as becomes evident from inspection of Fig. 2. A very pronounced minimum for both r_P and r_{DE} is found for a Ru-O spacing $Z_{ox} = 1.52 \pm 0.03 \text{ \AA}$; while the other minima for larger distances are much poorer and are hence without significance.

The resulting structure for the Cs-O-Ru(0001)- $(\sqrt{3} \times \sqrt{3})R30^\circ$ coadsorbate phase is reproduced in Fig. 1. The quoted error bars for the structural parameters result from an assumption of 95% reliability taking into account statistical errors only as proposed by Pendry.¹² Both the Cs and O atoms are located in hcp sites with respect to the Ru(0001) substrate lattice. With respect to the positions of the Cs atoms, the O atoms are in threefold sites below the plane formed by the alkali-metal adlayer. The Cs-Ru layer spacing of $3.04 \pm 0.07 \text{ \AA}$ corresponds to a hard sphere radius of the Cs atoms of $2.08 \pm 0.05 \text{ \AA}$, a value which is smaller by 0.08 \AA than that in the corresponding oxygen-free Cs overlayer structure.⁴ The Ru-O layer spacing is derived to be $1.52 \pm 0.03 \text{ \AA}$. The positions of the Ru atoms were found to be unchanged, that means lateral and vertical displacements of the substrate atoms led to no further improvement of the structural refinement. The symmetry of the structure is $p3$ and consequently two domains must exist due to the $p3m$ symmetry of the substrate. The existence of ordered domains is assumed from the observation of diffraction spots which appeared bright and narrow.

The intensity spectra for this best fit geometry is displayed in Fig. 3. The corresponding r factors are $r_{DE} = 0.33$ and $r_P = 0.31$.

Apart from being consistent with the quoted work-function data, the presented structural model is further supported by results from other experimental techniques: Metastable deexcitation spectroscopy probes the valence electronic properties of the outermost atomic layer and indeed exhibits no evidence for spectral features derived from O $2p$ levels (in contrast to ultraviolet photoemission spectroscopy), signaling that the O atoms are "buried" below the Cs atoms.¹⁶ High-resolution electron-energy-loss spectroscopy exhibits a peak at $25 \pm 3 \text{ meV}$ which was attributed to a Cs-O bending-mode type of vibration.¹⁷ The operation of strong interactions between the adsorbed Cs and O atoms is also reflected by the substantial increase of the desorption temperature for Cs in the presence of coadsorbed O.

The Cs-O separation in the coadsorption phase is $3.11 \pm 0.04 \text{ \AA}$ and thus somewhat larger than the bond lengths in (bulk) cesium oxides which range between 2.7 and 3.0 \AA . The same holds for the Cs-Cs separation of 4.7 \AA if compared with the values ranging between 3.6 and 4.4 \AA for the cesium suboxides.^{18,19} Both effects obviously signal the importance of strong interactions with the Ru substrate.

The Ru-O bond length for oxygen chemisorbed on Ru(0001) of 2.03 \AA (Ref. 20) is, on the other hand, sig-

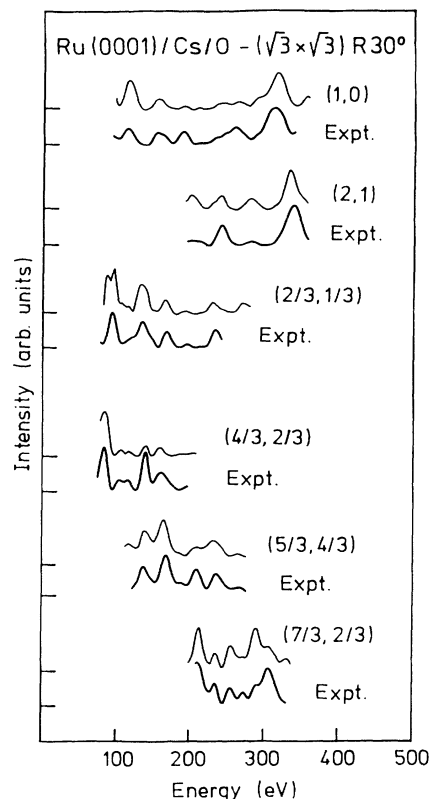


FIG. 3. Comparison of the experimental and calculated best fit $I(E)$ spectra ($r_P = 0.31$; $r_{DE} = 0.33$).

nificantly shorter than the corresponding value of 2.16 \AA with the present system which reflects a weaker interaction between O and Ru in the presence of coadsorbed Cs. The adsorption site of oxygen exhibits an enhanced charge density induced by the Cs overlayer, as expected by comparison with calculated charge-density distribution of the structurally equivalent Na/Al(111)- $(\sqrt{3} \times \sqrt{3})R30^\circ$ system with Na residing in a threefold hollow site.²¹ The increase of the hard-sphere radius of oxygen may be rationalized in terms of a net transfer of electronic charge from Cs (probably via the Ru substrate) to O. This effect, in turn, gives rise to the observed reduction of 0.1 \AA of the effective Cs radius from 2.2 \AA in the Cs/Ru(0001)- $(\sqrt{3} \times \sqrt{3})R30^\circ$ phase to 2.1 \AA with the coadsorbate phase. [It should be noted that the geometry of the Cs adsorption site is not altered, in contrast to the situation with the Cs/Ru(0001)- 2×2 phase for which the transition to on-top site occupancy is associated with a 0.3 \AA variation of the bond length.⁴]

In conclusion, LEED analysis provided a model for the structure of the Cs-O/Ru(0001)- $(\sqrt{3} \times \sqrt{3})R30^\circ$ phase which is consistent with all other available experimental evidence as well as with arguments derived from theoretical considerations and which may be regarded as a prototype for the large variety of combined alkali metal plus oxygen overlayers on transition metal surfaces.

The authors gratefully acknowledge fruitful discussions with J. Neugebauer and technical assistance by E. Piltz.

*Permanent address: Deutsches Patentamt, D-8000 München, Federal Republic of Germany.

†Permanent address: Institut für Kristallographie und Mineralogie, Universität München, Theresienstrasse 41, D-8000 München 2, Federal Republic of Germany.

¹D. S. Villars and I. Langmuir, *J. Am. Chem. Soc.* **53**, 486 (1931); see, e.g., L. Surnev, in *Physics and Chemistry of Alkali Metal Adsorption*, edited by H. P. Bonzel, A. M. Bradshaw, and G. Ertl (Elsevier, Amsterdam, 1989), p. 173.

²G. Ertl, in *Catalytic Ammonia Synthesis*, edited J. R. Jennings (Plenum, New York, 1991), p. 109.

³S. Andersson and J. B. Pendry, *J. Phys. C* **9**, 2721 (1976).

⁴H. Over, H. Bludau, M. Skottke-Klein, G. Ertl, W. Moritz, and C. T. Campbell, *Phys. Rev. B* **45**, 8638 (1992).

⁵K. Heinz, *Prog. Surf. Sci.* **27**, 239 (1988).

⁶J. B. Pendry, *Low Energy Electron Diffraction* (Academic, New York, 1974).

⁷J. Rundgren and A. Salwén, *J. Phys. C* **7**, 4247 (1974); **9**, 3701 (1976).

⁸W. Moritz, *J. Phys. C* **17**, 353 (1983).

⁹S. Y. Tong, A. Maldonado, C. H. Li, and M. A. Van Hove, *Surf. Sci.* **94**, 73 (1980).

¹⁰G. Kleinle, J. Wintterlin, G. Ertl, R.-J. Behm, F. Jona, and W.

Moritz, *Surf. Sci.* **225**, 171 (1990).

¹¹G. Kleinle, W. Moritz, D. L. Adams, and G. Ertl, *Surf. Sci.* **219**, L637 (1989).

¹²J. B. Pendry, *J. Phys. C* **13**, 937 (1980).

¹³G. Kleinle, W. Moritz, and G. Ertl, *Surf. Sci.* **238**, 119 (1990).

¹⁴W. Moritz, H. Over, G. Kleinle, and G. Ertl, in *The Structure of Surfaces III*, edited by S. Y. Tong, M. A. Van Hove, and K. Takayanagi (Springer, Berlin, 1991), p. 128.

¹⁵M. Kiskinova, G. Rangelov, and L. Surnev, *Surf. Sci.* **172**, 57 (1986).

¹⁶A. Böttcher, R. Grobecker, A. Morgante, and G. Ertl (unpublished).

¹⁷H. Shi, K. Jacobi, and G. Ertl, *Surf. Sci.* **269/270**, 682 (1992).

¹⁸A. Simon, *Naturwissenschaften* **58**, 622 (1971).

¹⁹A. Simon and E. Westerbeck, *Z. Anorg. Allg. Chem.* **428**, 187 (1977).

²⁰M. Lindroos, H. Pfnür, G. Held, and D. Menzel, *Surf. Sci.* **220**, 43 (1983); **222**, 451 (1989).

²¹A. Schmalz, S. Arminpirooz, L. Becker, J. Haase, J. Neugebauer, M. Scheffler, D. R. Batchelor, D. L. Adams, and E. Bøgh, *Phys. Rev. Lett.* **67**, 2163 (1991); J. Neugebauer (private communication).